2019 SECED Conference
Earthquake risk and engineering towards a resilient world
9-10 September 2019, Greenwich, London

UNDERSTANDING INDUCED SEISMICITY HAZARD RELATED TO SHALE GAS EXPLORATION IN THE UK

Gemma CREMEN[1], Maximilian J. WERNER[2] & Brian BAPTIE[3]

Abstract: *This study examines the seismic hazard associated with shale gas exploration in the UK, where such industrial activity is relatively new. We focus on the Preston New Road site in Lancashire, where shale gas exploration occurred in late 2018. We compile, process, and analyse ground motion data from nine seismometers located within 25 km of the site, which detected 57 exploration-related events with local magnitude (M_L) range -0.9 to 1.6. We use the data to test a number of pre-existing ground motion prediction equations for suitability to modelling potentially felt events induced by UK shale gas exploration: (1) the Akkar et al. (2014a) equations for European seismicity, (2) the Douglas et al. (2013) equation, developed for induced seismicity in geothermal areas, and (3) the Atkinson (2015) equation, developed for induced seismicity in eastern North America. We find that the Douglas et al. (2013) equation is the most suitable, at least for the considered ground motion intensity measures, although it can over-estimate ground motion variability. To understand if the ground motions differ relative to comparable motions from other types of UK seismicity, we compare the ground motion intensities observed with those recorded during a sequence of earthquakes near Newdigate, Surrey (believed to be natural) and a sequence of events near New Ollerton, Nottinghamshire (induced by coal-mining). We find that – depending on the intensity measure – the intensities are similar to or higher than those of the Newdigate sequence and are similar to or lower than those of the New Ollerton sequence.*

Introduction

Shale gas exploration can be a source of concern for local populations and policy makers (Williams et al. 2017), as the associated process of hydraulic fracturing may be accompanied by microseismicity (i.e. events with M_L<2.0 or otherwise too small to be felt) and, in some locations, small to moderate earthquakes that have the potential to cause damage to nearby buildings and infrastructure (Atkinson et al. 2016). The purpose of this study is to help improve understanding of the seismic hazard associated with shale gas exploration in the UK, where it is a relatively new industrial activity; the first well to specifically test for UK shale gas was drilled in 2010 (Selley, 2012), and the first recorded instance of seismicity induced by hydraulic fracturing in the UK occurred in 2011 (Clarke et al. 2014). We specifically focus on the Preston New Road (PNR) shale gas site near Blackpool in Lancashire (Figure 1), where hydraulic fracture operations were carried out between October and December 2018. We compile, process, and analyse ground motion data from nine seismometers, deployed within 25 km of the site to monitor seismicity. The seismometers detected 57 seismic events related to exploration operations in total, with M_L ranging from -0.9 to 1.6.

An essential component of understanding seismic hazard in a region is the ability to predict the level of ground shaking (and its associated uncertainty) at a given distance from a particular magnitude event, using ground motion prediction equations (GMPEs). While the magnitudes of the PNR events are significantly lower than those considered in typical seismic hazard analyses, GMPEs are still useful for assessing whether the associated shaking has the potential to be felt. We use the PNR data to test a number of pre-existing GMPEs for suitability to modelling the ground motions induced by UK shale gas exploration: (1) the Akkar et al. (2014a) equations, developed for European seismicity, (2) the Douglas et al. (2013) equation, developed for induced seismicity in geothermal areas, and (3) the Atkinson (2015) equation, developed for induced seismicity in eastern North America. Evaluation of the GMPEs is specifically carried out

[1] Research Associate, University of Bristol, Bristol, United Kingdom, gemma.cremen@bristol.ac.uk
[2] Senior Lecturer, University of Bristol, Bristol, United Kingdom
[3] Project Leader in Seismology, British Geological Survey, Edinburgh, United Kingdom

for peak ground velocity (PGV), peak ground acceleration (PGA), and 5% damped spectral accelerations at periods of 0.05s, 0.1s, and 0.2s ($SA_{0.05}$, $SA_{0.1}$, and $SA_{0.2}$ respectively).

It is also important to understand whether the seismic hazard associated with UK shale gas exploration differs relative to that associated with other types of UK seismicity. To achieve this, we compare the ground motions produced by PNR earthquakes to ground motions produced by similar magnitude events at similar depths in the 2018-2019 sequence of earthquakes near Newdigate, Surrey, which is believed to be naturally occurring (Verdon et al. 2019), and the 2013-2014 sequence of events near New Ollerton, Nottinghamshire, which was induced by coal-mining at the Thoresby Colliery (Verdon et al, 2017).

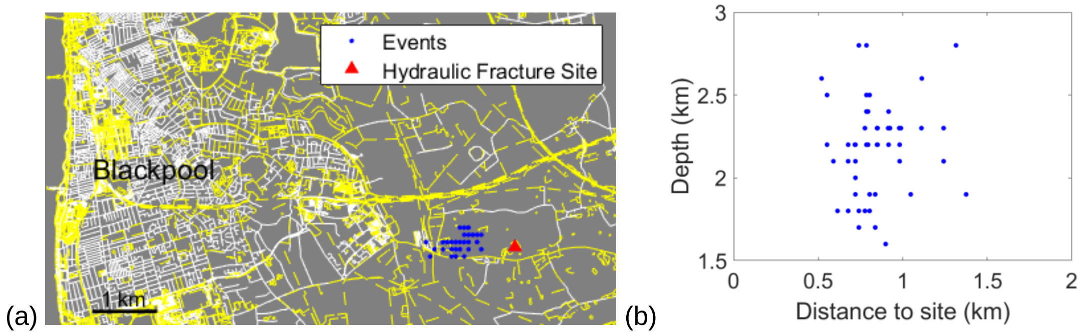

Figure 1. (a) Locations and (b) depths of earthquake events related to hydraulic fracturing at the PNR shale gas site, near Blackpool in Lancashire.

GMPE Evaluation Methodology

GMPEs Examined

We evaluate the suitability of various GMPEs for modelling the ground motions induced by hydraulic fracture operations at the PNR site: (1) Akkar et al. (2014a, hereafter ASB14), (2) Douglas et al. (2013, hereafter D13), and (3) Atkinson (2015, hereafter A15). ASB14 was chosen based on geographical relevance, while D13 and A15 were chosen for their application to induced seismicity.

ASB14 are a series of GMPEs developed for European and Middle East crustal seismicity that were derived using a subset of the Reference Database for Seismic Ground-Motion in Europe (RESORCE) (Akkar et al. 2014b). They are applicable for moment magnitudes (M_w) greater than 4 and distances less than 200 km. The equations use either point-source (i.e. epicentral and hypocentral distance) or finite-fault (surface projection of rupture distance) distance metrics. Events are sufficiently small such that rupture distance is not important in this study, so we only use the point-source equations (henceforth referred to as $ASB14_{hypo}$ and $ASB14_{epi}$).

D13 are a series of GMPEs developed for geothermal induced seismicity that were derived using data from induced and natural seismicity in Basel (Switzerland), Campi Flegrei (Italy), Geysers (United States), Hengill (Iceland), Roswinkel and Vorendaal (the Netherlands), and Soultz-sous-Forets (France). They are applicable for M_w greater than 1 and distances less than 50 km. All equations except one are site corrected to a reference rock condition (V_{s30}~=1100 m/s). This condition is significantly different to that observed at sites in this study (V_{s30}~=280 m/s, as explained in the 'Data' section), so we only use the uncorrected equation in this case.

A15 is a GMPE developed for induced seismicity in eastern North America that was derived using a subset of the Next Generation Attenuation-West 2 (NGA-West 2) database (Ancheta et al. 2014). It is applicable for magnitudes between 3 and 6 and distances less than approximately 50 km. The equation is site corrected to a reference soft rock condition (V_{s30} = 760 m/s), but the site correction model of Seyhan and Stewart (2014) can be used to apply the equation to other site conditions. We use this model to site correct our data.

Evaluation Criteria

Normalised log residuals are used to compare observed ground motions with those predicted from a given GMPE. A normalised log residual (z) for an observed ground motion amplitude, (im_{obs}) and the corresponding median ground motion amplitude predicted by a GMPE (im_{GMPE}) is computed as follows:

$$z = \frac{log(im_{obs}) - log(im_{GMPE})}{\sigma_T} \quad (1)$$

where σ_T is the total standard deviation of the GMPE and the base of the logarithm matches that used in the GMPE. Since GMPEs are described by lognormal distributions, normalised log residuals will follow a standard normal distribution (mean=0, standard deviation =1) if a GMPE is a perfect fit for the observed data. We specifically use the GMPE evaluation scheme developed by Scherbaum (2004), which ranks the suitability of the considered GMPEs based on summary statistics (i.e. mean, median, and standard deviation) of the normalised log residuals. The scheme also uses a likelihood-based goodness-of-fit measure (*LH*) that accounts for both model bias and the normality of the normalised log residuals. LH is calculated as follows:

$$LH = Erf\left(\frac{|z|}{\sqrt{2}}, \infty\right) = Erf(\infty) - Erf\left(\frac{|z|}{\sqrt{2}}\right) \quad (2)$$

where *Erf(x)* is the error function evaluated at *x*, and *z* is as defined in equation 1. *LH* values will be approximately uniformly distributed if the performance of a model is good. Each GMPE is assigned one of the following classifications by the scheme: (1) A - highest capability, (2) B - intermediate capability, (3) C - lowest accepted capability, or (4) D - unacceptable.

Since the data used in this study are dominated by records from individual earthquakes, we use the Stafford et al. (2007) modification to this ranking scheme, which evaluates inter-event (earthquake-to-earthquake differences at the same site) and intra-event (site-to-site differences for the same earthquake) residuals separately. The normalised log inter-event residual from the *i*th event ($z_{E,i}$) is calculated from Abrahamson and Youngs (1992):

$$z_{E,i} = \frac{\sigma_E \times \sum_j^{n_i} log(im_{obs,i,j}) - log(im_{GMPE,i,j})}{n_i\sigma_E^2 + \sigma_A^2} \quad (3)$$

where σ_E and σ_A are the GMPE's inter- and intra-event standard deviation respectively, n_i is the number of observations for the *i*th event, $im_{obs,i,j}$ is the *j*th observed ground motion amplitude for the *i*th event, and $im_{GMPE,i,j}$ is the corresponding median ground motion amplitude predicted from the GMPE. The normalised intra-event residual for the *j*th recording from the *i*th event ($z_{A,i,j}$) is calculated from:

$$z_{A,i,j} = \frac{log(im_{obs,i,j}) - log(im_{GMPE,i,j}) - z_{E,i}\sigma_E}{\sigma_A} \quad (4)$$

where all variables are as defined previously.

Data

We only examine data from the 16 detected PNR events with M_L>0 in this study, since smaller magnitude events have extremely low levels of shaking that will not be felt. 47 recordings are available from the nine seismometers for these events. The seismometers are 3-component Guralp 3-ESP.

We retrieve the raw waveforms and phase data recorded for these events from the BGS website (BGS, 2019). We convert the waveforms from dimensions of digital counts to velocity using the procedure of Haney et al. (2012) (for broadband seismometers), assuming a causal third-order high-pass Butterworth filter with frequency 3 Hz, a causal fifth-order low-pass Butterworth filter with frequency 20 Hz, and an oversampling rate of 5. Accelerations are then obtained by numerically differentiating the velocities. Spectral accelerations are computed using the algorithm provided in Wang (1996).

Ground motion intensities are calculated across a time window from p-wave arrival to 5 seconds after the occurrence of the maximum displacement amplitude. The value of a ground motion intensity measure used for a particular event and distance combination depends on the requirements of the GMPE of interest. For $ASB14_{hypo}$, $ASB14_{epi}$, and D13, it is taken as the geometric mean of the values computed for the two horizontal components. For A15, it is taken as the median value for the two horizontal components computed over all nonredundant azimuths, as detailed in Boore (2010). M_L values are converted to M_w values using the empirical relationship derived by Butcher et al. (2019) for coal-mining induced seismicity in the UK:

$$M_W = 0.69\, M_L + 0.74 \tag{5}$$

All sites sit on alluvial soils so we use a V_{S30} value of 280 m/s, the median value found for these types of soil by Campbell et al. (2016), for site correction factors in $ASB14_{hypo}$, $ASB14_{epi}$, and A15. We assume a linear site response for A15. We assume strike-slip style-of-faulting for $ASB14_{hypo}$ and $ASB14_{epi}$, as this is the dominant regime in the region (Felgett et al. 2018).

We compare PNR ground motion intensities to those recorded during similar magnitude events in both the 2018-2019 Newdigate, Surrey, earthquake sequence and the 2013-2014 New Ollerton, Nottinghamshire, earthquake sequence. We only examine recordings at distances less than 50 km, given the extremely low levels of shaking that occur beyond this distance for the considered magnitudes.

We consider the 14 earthquakes greater than 0 M_L that occurred in the Newdigate earthquake sequence before 15th February 2019, for which there are 18 recordings available within 50km from five 3-component broadband seismometers (all Guralp 3-ESP). We consider the 94 earthquakes greater than 0 M_L that occurred in the New Ollerton sequence, for which there are 210 recordings available within 50 km from five 3-component broadband seismometers (four are Guralp 3-ESP and one is a Guralp CMG3-T). Waveforms are accessed, corrected and filtered for both earthquake sequences using the criteria outlined previously. The data considered for all earthquake sequences are summarised in Figure 2.

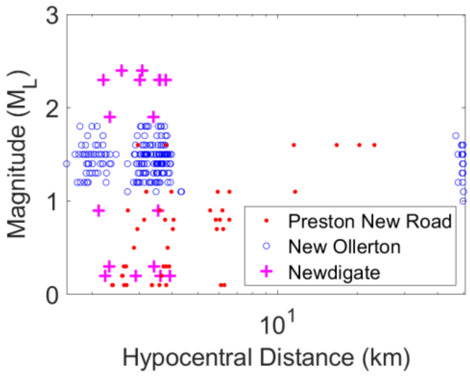

Figure 2. Magnitudes and hypocentral distances of the data considered for the PNR microseismicity. The data, recorded by the BGS, include 47 observations from 16 M_L>0 events. Also shown are magnitudes and hypocentral distances of the data considered for the 2018-2019 Newdigate earthquake sequence (18 observations from 14 M_L>0 events) and the 2013-2014 New Ollerton earthquake sequence (210 observations from 94 M_L>0 events).

GMPE Evaluation Results

Histograms of normalised log inter- and intra-event residuals for the four considered GMPEs and the PNR data are shown in Figure 3 (for PGV) and Figure 4 (for $SA_{0.05}$), along with the standard normal distribution that would be expected for a perfectly calibrated model. It can be seen that the predictions of $ASB14_{hypo}$, $ASB14_{epi}$, and A15 are biased in all cases; the mean of the normalised log residuals associated with both $ASB14_{hypo}$ and $ASB14_{epi}$ are less than 0 (implying over-prediction of the observed ground motions), while the mean of the normalised residuals associated with A15 are greater than 0 (implying under-prediction of the observed ground motions). Since all three GMPEs were calibrated at much higher magnitudes than those that occurred at the PNR site, these findings provide further support for previous studies (e.g. Bommer et al., 2007), which found that GMPEs derived from larger-magnitude events should not be extrapolated to predict ground motions from earthquakes with smaller magnitudes. The normalised log residuals associated with D13 are effectively unbiased in all cases, suggesting this GMPE is a good fit for modelling the PNR ground motions, although the residuals have lower variability than would be expected from a standard normal distribution.

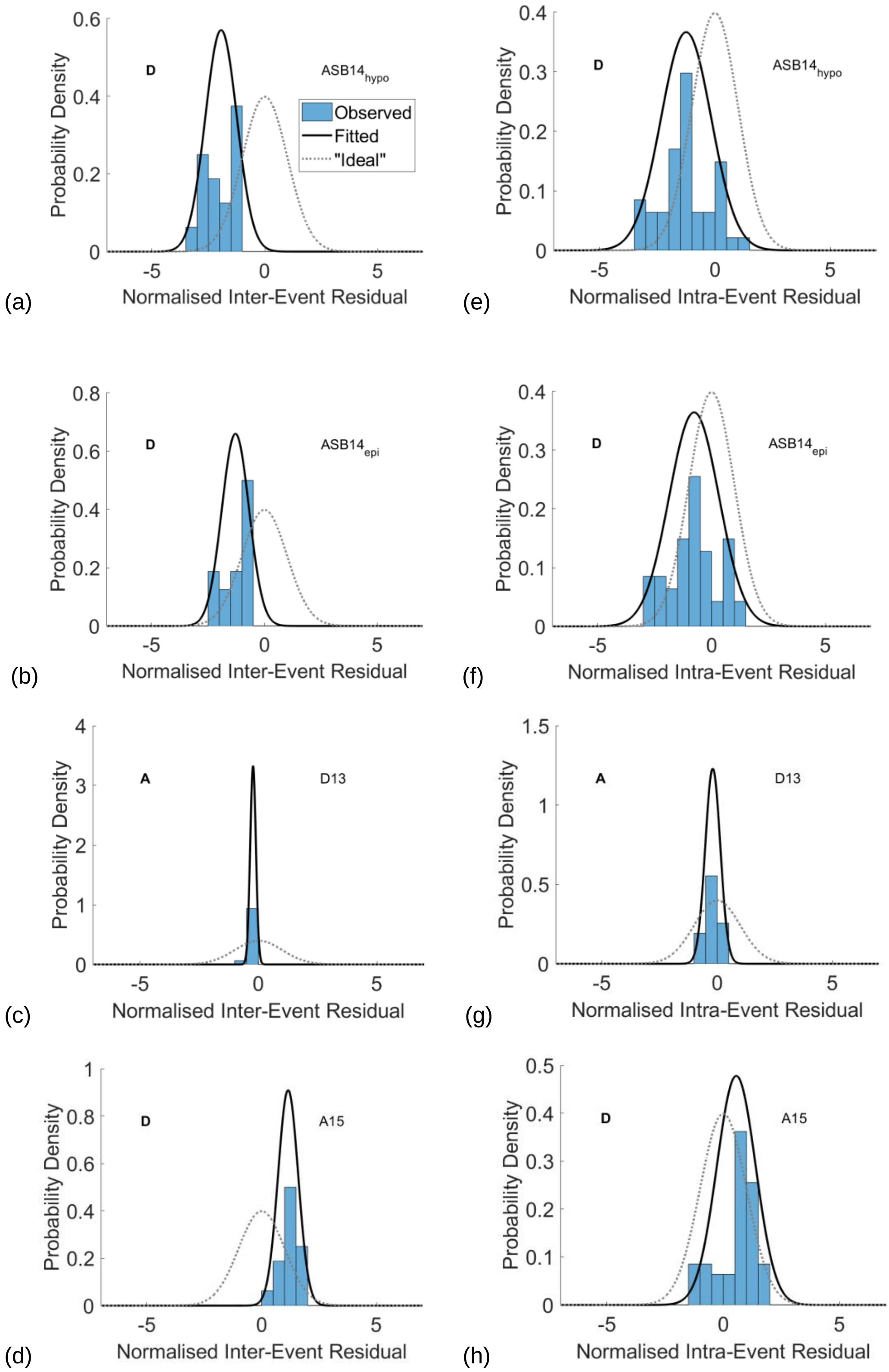

Figure 3. Histograms of the normalised log (a-d) inter-event and (e-h) intra-event residuals for PGV. The plots also include the normal distribution fitted to the residuals (solid black line) and the standard normal distribution (dashed grey line). Letters in bold indicate the GMPE capability class assigned by the Scherbaum et al. (2004) ranking scheme.

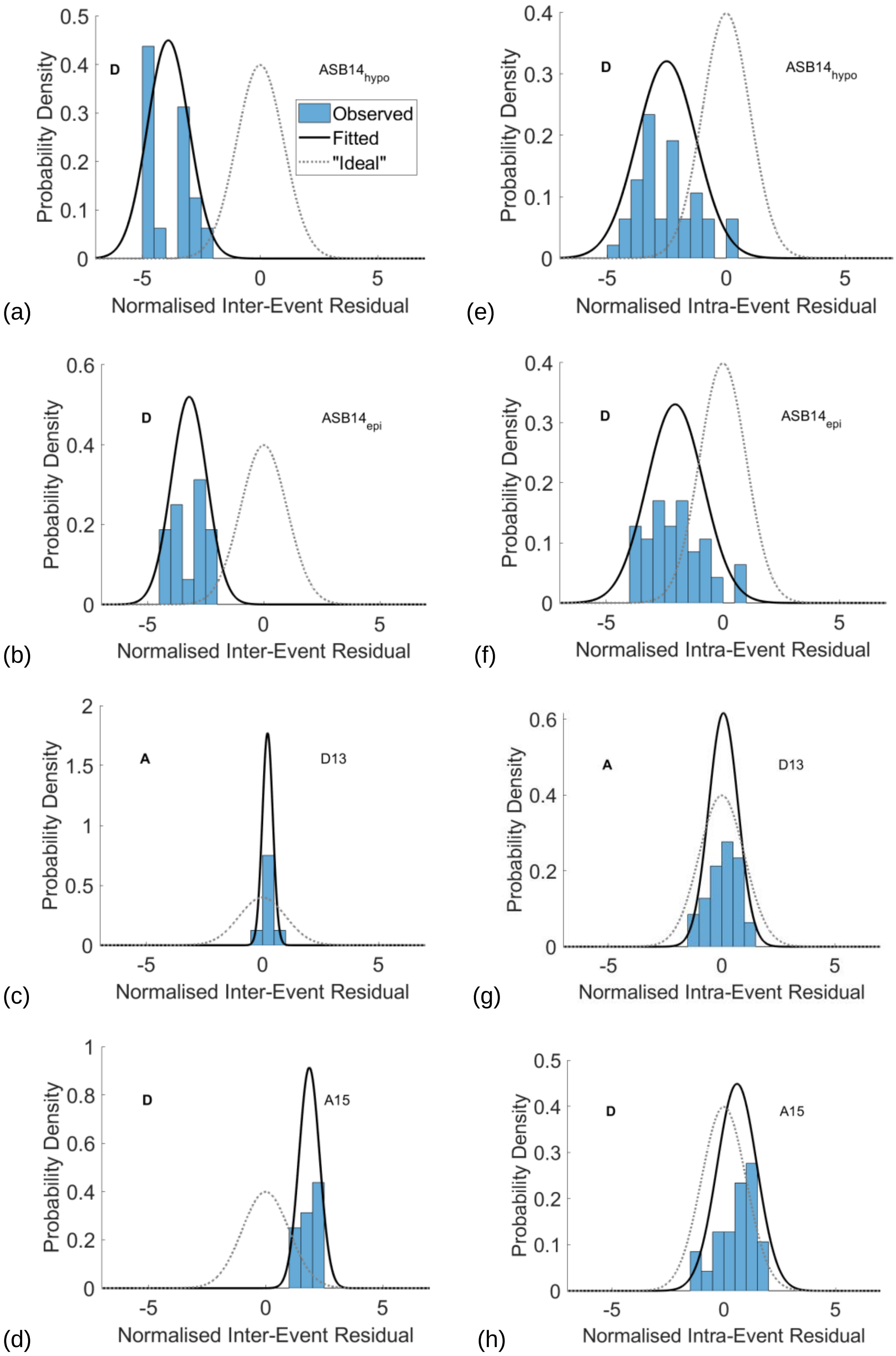

Figure 4. Histograms of the normalised log (a-d) inter-event and (e-h) intra-event residuals for $SA_{0.05}$. The plots also include the normal distribution fitted to the residuals (solid black line) and the standard normal distribution (dashed grey line). Letters in bold indicate the GMPE capability class assigned by the Scherbaum et al. (2004) ranking scheme.

Relevant summary statistics and the classifications assigned to the GMPEs by the Scherbaum (2004) ranking scheme are detailed in Table 1 (inter-event residuals) and Table 2 (intra-event residuals) for all ground motion intensity measures examined. Both $ASB14_{hypo}$ and $ASB14_{epi}$ are deemed unacceptable (classification D) for modelling any of the ground motion intensity measures examined. A15 is acceptable for modelling $SA_{0.2}$ and the intra-event variability of $SA_{0.1}$.

D13 is suitable for modelling all ground motion intensity measures examined (classifications A-C) and is in the highest two capability classes (A/B) for all cases except the inter-event variability of $SA_{0.2}$. (Note that the results obtained for $SA_{0.2}$ may be affected by low signal-to-noise ratio, which will be examined in future work). We can therefore conclude that, of the four GMPEs examined, D13 is the most suitable for modelling ground shaking due to hydraulic fracture operations at PNR, at least for the considered ground motion intensity measures and the limited available data. A comparison of the median PGV predictions of the four GMPEs with corresponding PNR data is included in Figure 5, for all magnitudes examined and a distance range of 3-4 km.

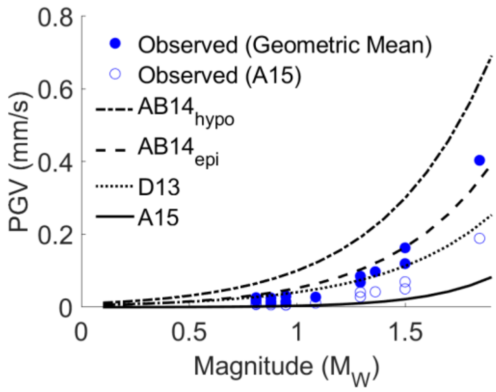

Figure 5. Median PGV predictions of the four GMPEs for a distance of 3.5 km, plotted against observed data within a 3-4km distance range, for all magnitudes examined. Note the observed data for A15 (open circles) is site-corrected and calculated differently to that for the other GMPEs (filled circles); see Data section for more details.

It is important to note, however, that while D13 is largely unbiased, the standard deviations of the normalised log inter-event residuals (σ_z) for D13 are extremely small, meaning D13 significantly over-predicts the observed inter-event variability. For example, σ_z = 0.1 for PGV inter-event residuals, which implies that the actual PGV inter-event variability is only 10% of that expected by D13. Thus, direct implementation of D13 for the PNR case may result in a notable overestimation of seismic hazard, particularly at long return periods (Restrepo-Valez and Bommer, 2003). This problem could be overcome by developing a PNR zone-specific inter-event variability for the model. However, the observed inter-event variability may be a function of the small number (16) of earthquakes examined and should be re-assessed as future earthquakes occur. Note that failure to penalise small values of σ_z is a known limitation of the Scherbaum (2004) ranking scheme (Bommer, 2007), and this should be kept in mind when using it as an evaluation tool.

IM	**$ASB14_{hypo}$**					**$ASB14_{epi}$**				
	L	M	E	σ_z	**R**	L	M	E	σ_z	**R**
PGA	0.0	-4.1	-4.1	1.0	**D**	0.0	-3.4	-3.4	0.8	**D**
PGV	0.1	-1.8	-1.9	0.7	**D**	0.3	-1.1	-1.3	0.6	**D**
$SA_{0.05}$	0.0	-3.9	-3.9	0.9	**D**	0.0	-3.1	-3.2	0.8	**D**
$SA_{0.1}$	0.0	-4.6	-4.8	0.9	**D**	0.0	-3,9	-4.1	0.7	**D**
$SA_{0.2}$	0.0	-5.3	-5.4	1.0	**D**	0.0	-4.6	-4.7	0.9	**D**
IM	**D13**					**A15**				
	L	M	E	σ_z	**R**	L	M	E	σ_z	**R**
PGA	0.8	0.2	0.2	0.2	**A**	0.1	1.7	1.7	0.4	**D**
PGV	0.8	-0.2	-0.2	0.1	**A**	0.3	1.1	1.2	0.4	**D**
$SA_{0.05}$	0.8	0.2	0.2	0.2	**A**	0.0	2.0	1.9	0.4	**D**
$SA_{0.1}$	0.7	0.4	0.4	0.2	**B**	0.2	1.4	1.4	0.3	**D**
$SA_{0.2}$	0.5	0.6	0.6	0.2	**C**	0.9	0.2	0.2	0.2	**A**

Table 1. Ranking GMPEs using the Scherbaum et al. (2004) classification scheme for inter-event residuals. Note the following abbreviations used: IM = intensity measure, L = median value of LH, M = median normalised log inter-event residual, E = mean normalised log inter-event residual,
σ_z = standard deviation of the normalised log inter-event residuals, R = GMPE capability class assigned by the scheme.

IM	ASB14hypo					ASB14epi				
	L	M	E	σ_z	R	L	M	E	σ_z	R
PGA	0.0	-2.9	-2.6	1.2	**D**	0.0	-2.2	-2.1	1.2	**D**
PGV	0.2	-1.2	-1.3	1.1	**D**	0.4	-0.6	-0.8	1.1	**D**
$SA_{0.05}$	0.0	-2.6	-2.5	1.2	**D**	0.0	-2.2	-2.0	1.2	**D**
$SA_{0.1}$	0.0	-3.0	-2.8	1.2	**D**	0.0	-2.4	-2.3	1.1	**D**
$SA_{0.2}$	0.0	-3.7	-3.3	1.1	**D**	0.0	-3.2	-2.8	1.0	**D**
IM	**D13**					**A15**				
	L	M	E	σ_z	R	L	M	E	σ_z	R
PGA	0.7	0.0	0.1	0.6	**A**	0.3	1.0	0.7	0.9	**D**
PGV	0.8	-0.2	-0.2	0.3	**A**	0.4	0.8	0.6	0.8	**D**
$SA_{0.05}$	0.6	0.1	0.1	0.6	**A**	0.3	0.9	0.6	0.9	**D**
$SA_{0.1}$	0.6	0.2	0.2	0.6	**A**	0.5	0.6	0.6	0.8	**C**
$SA_{0.2}$	0.6	0.4	0.3	0.5	**B**	0.7	0.1	0.1	0.5	**A**

Table 2. Ranking GMPEs using the Scherbaum et al. (2004) classification scheme for intra-event residuals. Abbreviations are as defined in Table 1, but for intra-event residuals.

Comparing Ground Motions from Different Types of UK Seismicity

To understand if the ground motions from shale gas-related seismicity differ relative to ground motions from other types of UK seismicity, we compare the ground motion intensities observed in the PNR sequence with those observed in the 2018-2019 Newdigate earthquake sequence in Surrey, which is believed to be naturally occurring, and those observed in the 2013-2014 New Ollerton earthquake sequence in Nottinghamshire, which was induced by coal-mining. Comparisons are carried out using the mean normalised log inter- and intra-event residuals calculated for D13 (from equations 3 and 4). The use of residuals enables comparisons to be carried out without (explicit) consideration of either magnitude or distance. Figure 6 shows the mean normalised log residuals across the three earthquake sequences, for all ground motion intensity measures examined.

It can be seen that both the mean normalised log inter- and intra-event residuals associated with the Newdigate earthquake sequence are similar to those associated with the other two sequences for three of the five ground motion intensity measures examined: PGV, PGA, and $SA_{0.05}$. However, the residuals of the naturally occurring sequence are notably smaller than those of the induced earthquake sequences for $SA_{0.1}$ and $SA_{0.2}$, implying that the induced sequences produce higher ground motion intensities than the naturally occurring sequence for these intensity measures. The mean residuals are similar for both induced earthquake sequences across all ground motion intensity measures except $SA_{0.2}$, for which the mean inter-event residual associated with the New Ollerton earthquake sequence is notably higher than that associated with PNR. This means that $SA_{0.2}$ values associated with New Ollerton earthquakes are consistently larger than those associated with PNR events.

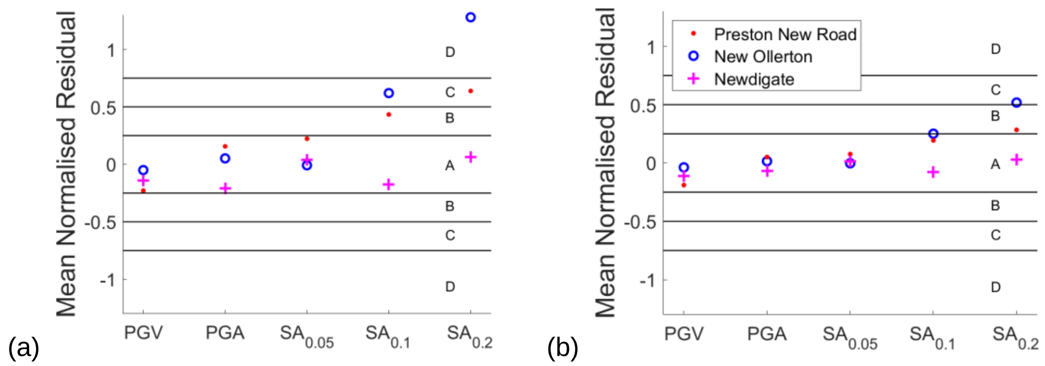

Figure 6. Mean normalised log (a) inter-event and (b) intra-event residuals for the different earthquake sequences and all ground motion intensity measures examined. Solid black lines indicate the boundaries between the Scherbaum et al. (2004) classifications (bold letters).

We can conclude that there are differences in the ground motions from earthquakes related to UK shale gas exploration and those from earthquakes related to other types of UK seismicity. Differences between the induced seismicity types are sufficient to affect the suitability of D13 for modelling ground motions (Figure 6); D13 is acceptable for all considered ground motion intensity measures in the case of shale-gas related seismicity, but (based on the mean of normalised log residuals alone) it is not acceptable for modelling $SA_{0.2}$ in the case of the coal-mining induced New Ollerton earthquake sequence. It is important to keep in mind, however, that these conclusions are based on limited data (less than 300 recordings across the three earthquake sequences). They may also be an artefact of the geographic separation of the different seismicity types; we are not comparing the earthquakes under identical conditions.

Conclusions

Shale gas exploration can be a source of concern for local stakeholders, as it may lead to microseismicity and, in some cases, small to moderate earthquakes with the potential to cause damage to buildings and infrastructure. This study has focused on improving understanding of the seismic hazard associated with shale gas exploration in the UK, where operations are at a relatively early stage. We specifically focused on the PNR site near Blackpool in Lancashire, where shale gas exploration occurred in late 2018. We compiled, processed, and analysed ground motion data recorded within 25 km of the site during 16 M_L >0 events related to operations.

We evaluated the suitability of four GMPEs for the region ($ASB14_{hypo}$, $ASB14_{epi}$, D13, and A15), using the modified Scherbaum (2004) ranking scheme outlined in Stafford et al. (2007). We found that D13 was the most suitable GMPE of the four, at least for the considered ground motion intensity measures of PGV, PGA, $SA_{0.05}$, $SA_{0.1}$, and $SA_{0.2}$ and the small dataset of observed recordings available. However, while D13 is unbiased with respect to the PNR data, it tends to significantly overestimate the inter-event variability. This implies that D13 would overestimate the seismic hazard, particularly at long return periods, if the GMPE was directly implemented in calculations. This problem could be overcome by developing a zone-specific inter-event variability for the model. Note that the observed inter-event variability may be a function of the small number of earthquakes examined and should be re-assessed as future earthquakes occur.

To understand if the ground motions from shale gas-related seismicity differ relative to ground motions from other types of UK seismicity, we compared PNR ground motion intensities to those recorded during similar magnitude events in both the 2018-2019 Newdigate, Surrey earthquake sequence (believed to be naturally occurring) and the 2013 New Ollerton, Nottinghamshire earthquake sequence (induced by coal-mining). We found that there were differences between the ground motion intensities obtained for the different types of seismicity across certain intensity measures; the naturally occurring earthquakes had lower intensity values than those of the induced events for $SA_{0.1}$ and $SA_{0.2}$, while $SA_{0.2}$ values for the New Ollerton earthquake sequence were consistently higher than those of the PNR events. It was also found that D13 is not as suitable for modelling coal-mining induced UK seismicity as it is for modelling UK shale gas-related seismicity. It is important to keep in mind however, that these conclusions are based on limited data. They may also be an artefact of the geographic separation of the different seismicity types; we did not compare the earthquakes under identical conditions.

The findings of this study ultimately enhance understanding of the implications of induced seismicity related to UK shale gas exploration, and have many potential uses in further related studies. For example, they could be used to inform the development of a risk framework for decision-making related to UK regulations on such operations.

References

Abrahamson NA and Youngs RR (1992), A stable algorithm for regression analyses using the random effects model, *Bulletin of the Seismological Society of America*, 82(1): 505-510

Akkar S, Sandikkaya MA, Bommer JJ (2014a), Empirical ground-motion models for point- and extended-source crustal earthquake scenarios in Europe and the Middle East, *Bulletin of Earthquake Engineering*, 12: 359-387

Akkar S, Sandikkaya MA, Seyurt M, Azari Sisi A, Ay BO, Traversa P, Douglas J, Cotton F, Luzi L, Hernandez B, Godey S (2014b), Reference database for seismic ground-motion in Europe (RESORCE), *Bulletin of Earthquake Engineering*, 12: 311-399

Ancheta TD, Darragh RB, Stewart JP, Seyhan E, Silva WJ, Chiou BSJ, Wooddell KE, Graves RW, Kottke AR, Boore DM, Kishida T, and Donahue JL (2014), PEER NGA-West2 database, *Earthquake Spectra*, 30(3): 989-1006

Atkinson GM (2015), Ground-motion prediction equation for small-to-moderate events at short hypocentral distances, with application to induced-seismicity hazards, *Bulletin of the Seismological Society of America*, 105(2A): 981-992

Atkinson GM, Eaton DW, Ghofrani H, Walker D, Cheadle B, Schultz R, Scherbakov R, Tiampo K, Gu J, Harrington RM, Liu Y, van der Baan M, and Kao H (2016), Hydraulic fracturing and seismicity in the western Canada sedimentary basin, *Seismological Research Letters*, 87(3): 631-647

BGS (2019), British Geological Survey Official Website. Available at: https://www.bgs.ac.uk/ (Accessed February and March 2019)

Bommer JJ, Stafford PJ, Alarcón JE, Akkar S (2007), The influence of magnitude range on empirical ground-motion prediction, *Bulletin of the Seismological Society of America*, 97(6): 2152-2170

Boore DM (2010), Orientation-independent, nongeometric-mean measures of seismic intensity from two horizontal components of motion, *Bulletin of the Seismological Society of America*, 100(4): 1830-1835

Butcher A, Luckett R, Kendall J-M, Baptie, BJ (2019), Corner frequencies, seismic moments and earthquake magnitudes: The effects of high-frequency attenuation on microseismicity, *Bulletin of the Seismological Society of America*, submitted

Campbell N, Fenton C, and Tallett-Williams S (2016), An investigation into the effects of material properties on shear wave velocity in rocks/soils. *Proceedings of the 5th International Conference on Geotechnical and Geophysical Site Characterization ISC-5, Gold Coast, Australia, 5-9 September 2016*

Clarke H, Eisner L, Styles P, and Turner P (2014), Felt seismicity associated with shale gas hydraulic fracturing: The first documented example in Europe, *Geophysical Research Letters*, 41(23): 8308-8314

Douglas J, Edwards B, Convertito V, Sharma N, Tramelli A, Kraaijpoel D, Cabrera BM, Maercklin N, and Troise C, (2013), Predicting ground motions from induced earthquakes in geothermal areas, *Bulletin of the Seismological Society of America*, 103(3): 1875-1897

Fellgett MW, Kingdon A, Williams JDO, and Gent CMA (2018), Stress magnitude across UK regions: new analysis and legacy data across potentially prospective unconventional resource areas, *Marine and Petroleum Geology*, 97: 24-31

Haney MM, Power J, West M, and Michaels P (2012), Causal instrument corrections for short-period and broadband seismometers, *Seismological Research Letters*, 83(5): 834-845

Restrepo-Velez LF and Bommer, JJ (2003), An exploration of the scatter in ground-motion prediction equations and the implications for seismic hazard assessment, *Journal of Earthquake Engineering*, 7(sup001): 171-199

Scherbaum F, Cotton F, and Smit P (2004), On the use of response spectral-reference data for the selection and ranking of ground-motion models for seismic-hazard analysis in regions of moderate seismicity: The case of rock motion, *Bulletin of the Seismological Society of America*, 94(6): 2164-2185

Selley RC (2012), UK shale gas: The story so far, *Marine and Petroleum Geology*, 31(1): 100-109

Seyhan E and Stewart JP(2014), Semi-empirical nonlinear site amplification from NGA-West2 data and simulations, *Earthquake Spectra*, 30(3): 1241-1256

Stafford, PJ, Strasser FO, Bommer JJ (2008), An evaluation of the applicability of the NGA models to ground-motion prediction in the Euro-Mediterranean region, *Bulletin of Earthquake Engineering*, 6: 149-177

Verdon JP, Kendall J-M, Butcher A, Luckett R, and Baptie BJ (2017), Seismicity induced by longwall coal mining at the Thoresby Colliery, Nottinghamshire, UK, *Geophysical Journal International,* 212(2): 942-954

Verdon JP, Baptie BJ, and Bommer, JJ (2019), An improved framework for discriminating seismicity induced by industrial activities from natural earthquakes, *Seismological Research Letters,* (in press)

Wang L-J (1996), *Processing of near-field earthquake accelerograms*, Report No. EERl 96-04, California Institute of Technology, USA

Williams L, Macnaghten P, Davies R, Curtis S (2017), Framing 'fracking': Exploring public perceptions of hydraulic fracturing in the United Kingdom, *Public Understanding of Science*, 26(1): 89-104